J. COMBIN. MATH. COMBIN. COMPUT. 127b (2025) 8701--8721

Journal of Combinatorial Mathematics and Combinatorial Computing
www.combinatorialpress.com/jcmcc

Performance assessment and optimization strategy of new energy distribution network fault self-healing system based on Monte Carlo simulation

Yuan Wen[1], Zhongqiang Zhou[2,✉], Yixin Xia[3], Ying Lu[4], Jun Ao[5]

[1] Power Supply Bureau, Guizhou Power Grid Dispatching Control Center, Kaili, Guizhou, 556000, China
[2] Automation Department, Guizhou Power Grid Dispatching Control Center, Guiyang, Guizhou, 550000, China
[3] Bijie Power Supply Bureau, Guizhou Power Grid Dispatching Control Center, Bijie, Guizhou, 551700, China
[4] Zunyi Power Supply Bureau, Guizhou Power Grid Dispatching Control Center, Zunyi, Guizhou, 563000, China
[5] Automation Division, Guiyang Power Supply Bureau Dispatching Control Center, Guiyang, Guizhou, 550000, China

ABSTRACT

The distribution network system is directly connected to users, and its faults directly affect people's daily life and economic activities. In order to realize rapid fault location, isolation and self-healing, this paper carries out a new energy distribution system reliability assessment based on sequential Monte Carlo simulation algorithm. Comparing the use of sequential simulation algorithms, non-sequential simulation algorithms and pseudo-sequential simulation algorithms in the state analysis of distribution network systems, the sequential Monte Carlo method is selected to establish a simulation model for distribution network reliability assessment. According to the "2-3-6" architecture system commonly used in distribution networks, a new energy distribution network self-healing system data communication scheme is designed. The Monte Carlo simulation method is used to model and analyze the reliability of new energy coupled components and to evaluate the reliability indexes. The simulation environment is designed and the RTDS model is used to test the self-healing system of intelligent devices in the distribution network. In the new energy distribution network data scheme designed in this paper, the distribution network self-healing technology is able to remove the fault time within 95ms and complete the fault point elimination work. And when the DG can make the far power side and the switch is located in the near power side, the distribution self-healing system is able to remove the fault point within 60ms time and complete the self-healing operation of the distribution network fault.

Keywords: monte carlo, reliability assessment, fault self-healing, distribution network

✉ Corresponding author.
E-mail address: gzdwzzq@163.com (Z. Zhou).
Received 03 February 2024; Revised 12 April 2024; Accepted 10 November 2024; Published Online 16 April 2025.
DOI: 10.61091/jcmcc127b-478

1. Introduction

With the proposal of new energy strategy and further opening of grid operation mode, the power system scale is increasing and the structure is more complex, which poses new challenges to the reliability, proactivity, and environmental friendliness of the traditional centralized large-scale power grid. Especially at the distribution network, the large-scale access of distributed generation (DG) leads to a complicated grid topology network [1]. As the tail end of the power system directly connected to the users, when suffering from serious external disturbances (e.g., natural disasters, equipment failures, and demand/supply fluctuations), the failure to quickly restore power supply will bring great losses to the lives and properties of users [2]. The islanding effect of distributed power supplies plays an important role in the power grid, such as improving the system fault defense capability and maximizing the restoration of power supply. However, due to the intermittency and uncertainty of the output of major distributed generation (DG), such as photovoltaic and wind power, as well as the non-constant power of the users in the fault zone, the loads that can be met by the DG and the effectiveness of the restoration range of the power supply in each isolated power supply area made up of DGs after a fault are not certain [3-4]. In order to make the distribution network robust enough to restore power supply and avoid power interruption, the traditional solution is to increase the standby capacity of the DG, but according to the new energy policy of the country, the distribution network should solve the problem of efficient energy utilization and safe operation in a more economical and low-carbon way, and at the same time, the solution has both simplicity and reusability. Therefore, it is of great significance to comprehensively consider reliability, economy and other performance indicators in distribution network fault studies [5-7].

This paper proposes the basic process of power system reliability assessment and screens the power system reliability assessment indexes. It points out the scope of application of Monte Carlo simulation method, establishes the simulation model of distribution network reliability assessment by using sequential Monte Carlo method, and updates the operation process of Monte Carlo assessment method. Analyze the conditions to meet the self-healing conditions of distribution networks, and obtain the methods to determine and deal with transient faults and permanent faults. Analyze the construction of a sample new energy distribution network and design the data communication scheme and implementation technology of the distribution network self-healing system. Conduct Monte Carlo simulation of new energy distribution network system to analyze the reliability index of new energy distribution network under different system structures. Design the simulation environment to analyze the fault self-healing technology of new energy distribution network.

2. Overview

In view of the high incidence of faults in distribution networks, the development trend of grid intelligence puts forward new requirements for power system fault identification and localization, self-healing, and restoration of power supply methods. Literature [8] proposes an impedance-based fault localization method for intelligent distribution networks, and verifies the effectiveness of the method through simulation experiments, which has high fault localization accuracy and can determine the actual location of the fault. Literature [9] proposed a distribution network fault section identification and fault localization method based on artificial neural network, and the feasibility of the proposed method was verified by simulation experiments, while the neural network has a better processing effect on faults with different angles, different locations and different resistances. Literature [10] used real cases to point out that distributed generation (DG) can lead to adverse effects on short-circuit current and fault detection in distribution networks, exploring, and also examining the effect of PV DG on the response of protective devices in radial distribution networks. Literature [11] states that the success of state-of-the-art smart grid functionality is related to fault isolation, localization, and system restoration (FLISR)-related functions, and through the co-simulation of fault management and reconfiguration of smart distribution grids with Ite communications, it was found that in distribution grids, the long term evolution of the communication system, 4G, can be used as a medium of communication for advanced fault localization, elimination, and network reconfiguration. Literature [12] points out that the application of self-healing technology in distribution networks contributes to the correct and reliable operation of the grid, mainly discusses the current self-healing network validation techniques and summarizes their main aspects and lists in order to explore new research directions for self-healing technology in distribution networks. Literature [13] highlights the importance of self-healing control in smart grids and proposes the structure and control strategy of an advanced self-healing control system, aiming to self-heal any disturbances in the distribution system of smart grids, to realize the safe operation of distribution grids, and thus to improve the efficiency, resilience, continuity, and reliability of distribution grids.

In addition, literature [14] proposes an agent-based service restoration method for distributed generation smart distribution systems and verifies the effectiveness and feasibility of the altered method through simulation experiments, which can restore the unserved area after a fault. Literature [15] shows the self-healing dilemma faced in distributed systems, and proposes a novel and generalized method for modeling system operation fault scenarios, which is verified by a large number of experiments to accurately measure and predict the inconsistency generated by the poor results of error correction and fault tolerance, and can provide technical support for how distributed systems can adjust self-healing at an early stage. Literature [16] highlights the shortcomings of existing self-healing assessment of smart distribution networks, proposes a self-healing evaluation method for smart distribution networks based on entropy weight method and uncertainty theory for four quantitative indexes: self-healing credibility, self-healing rate, self-healing speed, and self-healing benefit of smart distribution networks, and verifies the effectiveness of the proposed method through numerical simulation. Literature [17] constructed a multi-intelligence body self-healing framework considering fault tolerance and automatic recovery of distribution networks, and a comprehensive simulation was carried out in bus distribution networks, and the results confirmed the scientific and applicability of the constructed framework, which is of great significance for the control and protection of distribution networks. Literature [18] proposed a stochastic method for assessing the self-healing capability of active islanded AC/DC hybrid microgrids based on Monte Carlo simulation, and designed simulated self-healing simulation experiments, and the results pointed out that distributed generation and flexible devices can improve the resilience of islanded microgrids, which can help to improve the self-healing capability of microgrids for faults. Literature [19] proposes a new self-healing strategy for distributed generator distribution grids considering uncertain power quality constraints, and the superior performance of the proposed strategy in terms of security, recovery capability and optimization efficiency is verified by a real distribution grid with 94 nodes, which can effectively improve the reliability of power supply in smart distribution grids.

3. Power system reliability assessment based on the Monte Carlo method

3.1. Basic process of power system reliability assessment

The power system reliability assessment is a comprehensive quantitative probabilistic assessment of the adequacy of the generation capacity and the adequacy of the transmission capacity of the main transmission network and its ability to meet the quality requirements as a point of load, taking into account the occurrence of random failures of transmission equipment and generation equipment [20-22].

The general process of power system reliability assessment is shown in Fig. 1, which mainly includes the following steps:

1) Firstly, input the data related to the current calculation and the data related to the component

outage.

2) Establish the component outage model based on the input corresponding data.

3) After selecting the sampling state, analyze the selected state.

4) Determine whether there is a problem with the system. If there is a problem with the system, corrective measures need to be taken immediately. If there is no problem with the system, jump directly to step 5).

5) Update the system indicators.

6) When the end conditions are met, the reliability indicators can then be output.

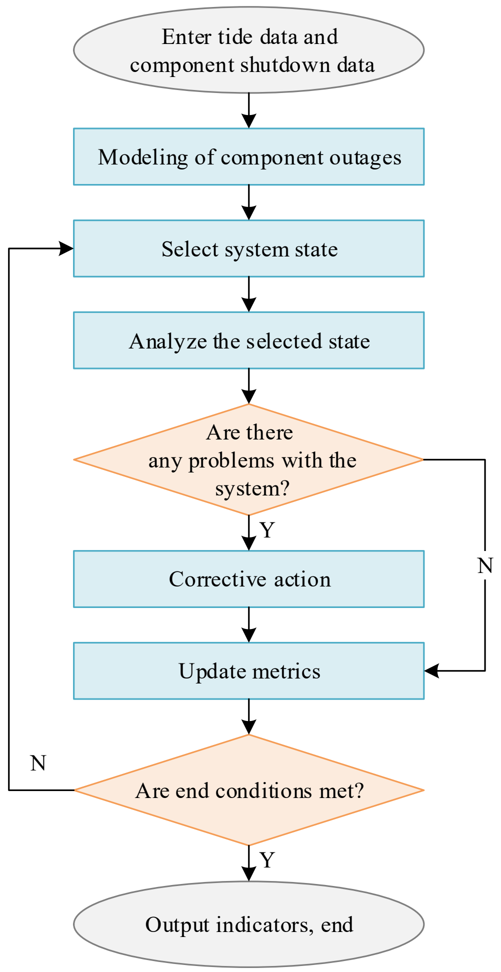

Fig. 1. The basic process of reliability evaluation of power system

3.2. Power System Reliability Indicators and Selection

After the modeling of the wind farm is completed, access to the power generation and transmission system is performed to carry out the system trend in each state and determine the system voltage offset in each state. Judge whether the system voltage will be unstable or the stability will change because of the difference of the accessed wind power and the different system nodes of the accessed WTGs.

Accurate reliability indicators can describe the reliability of the transmission and generation system, transmission and generation system reliability assessment is mainly through the relevant assessment methods to calculate the reliability indicators of the power system. The main reliability indicators of the power system are EDNS (Electricity Deficiency Expectation), LOLF (Load Shedding Frequency), LOLP (Load Shedding Probability), EENS (Electricity Shortage Expectation), LOLD (Load Shedding

Average Duration), and ROLV (Risk of Line Overloading).

Electricity Deficiency Expectation (EDNS) is used to describe the magnitude of its load curtailment expectation during the power system assessment and can be expressed in equation (1):

$$E_{DNS} = \oiint_{\Omega} F_{EDNS}(x)dx \tag{1}$$

where E_{DNS} is the magnitude of the power deficit expectation and $F_{EDNS}(x)$ represents the amount of load reduction of the system in state x.

The Load Reduction Frequency (LOLF) is used to describe the average number of times the power system experiences power deficiencies during the evaluated one-year time period and can be expressed in equation (2):

$$L_{OLF} = \oiint_{\Omega} F_{LOLF}(x)dx \tag{2}$$

where L_{OLF} denotes the magnitude of the load curtailment frequency. If load curtailment occurs while the power system is in state x, then the reliability function $F_{LOLF}(x) = 0$. otherwise $F_{LOLF}(x) = \sum_{i=1}^{N} \eta_i$, where η_i denotes the rate at which component i changes the state it is currently in.

The load curtailment probability (LOLP) describes the magnitude of the likelihood that load curtailment (i.e., power shortage) will occur during the evaluation period and can be expressed as:

$$L_{OLP} = \oiint_{\Omega} F_{LOLP}(x)dx \tag{3}$$

where L_{OLP} represents the magnitude of the load curtailment probability. If load curtailment occurs when the power system is currently in state x, then reliability function $F_{LOLP}(x) = 1$, otherwise $F_{LOLP}(x) = 0$.

Electricity Shortage Expectation (EENS), also known as Expected Shortage of Supply (ESS), is used to describe the amount of electricity lost by the power system due to load curtailment during the evaluation period.The relationship between EDNS and EENS can be expressed as:

$$E_{ENS} = E_{DNS} \times T \tag{4}$$

where E_{ENS} is the size of the EENS. T is the time span of the assessment.

Load curtailment average duration (LOLD), describes the average duration of the power system when load curtailment occurs.LOLD can be derived from LOLF and LOLP with the relationship:

$$L_{OLD} = \frac{L_{OLP} \times 8760}{L_{OLF}} \tag{5}$$

where L_{OLD} is the magnitude of the average duration of load curtailment.

The system outage power expectation ($EPNS$) represents the expected value of power loss due to insufficient system power supply with the relation:

$$EPNS = E(X - R), X > R \tag{6}$$

where X is the system shutdown capacity. R is the system standby capacity.

3.3. Monte Carlo method for distribution network reliability assessment

3.3.1. Monte Carlo simulation. Monte Carlo simulation is a method based on stochastic sampling simulation, the basic idea of which is to build a probabilistic model or a stochastic process so that its parameters are solutions to the problem to be solved. The model or process is then observed or sampled to calculate the statistical eigenvalues of the required parameters and use it as a numerical solution to the problem to be solved.

It has been shown that Monte Carlo simulation can be used to solve both stochastic and deterministic problems that can be transformed into probabilistic model solutions. Its greatest advantage lies in the fact that the convergence speed and accuracy of the computation are independent of the size of the system and the complexity of the problem, which makes it widely used in many engineering fields.

Suppose x is a random variable and the quantity to be estimated L is the expected value of the function $H(x)$ of the random variable:

$$L = E[H(x)] = \int_{\Omega} H(x) f(x) dx \tag{7}$$

where $f(x)$ is the probability density function of x on space Ω. According to the law of large numbers, when the sample size N is sufficiently large, the approximate estimate of Eq. (7) is:

$$L = \int_{\Omega} H(x) f(x) dx \approx \lim_{N \to \infty} \frac{1}{N} \sum_{i=1}^{N} H\left(x_i\right) \tag{8}$$

where $x_i (i = 1, 2, \cdots, N)$ is a sample of N random variables independently and identically distributed with $f(x)$ a probability density distribution. In practice, Monte Carlo simulations L are used by independently sampling a large number of random variables x according to the probability density function $f(x)$ for a sample $\left(x_1, \cdots, x_i, \cdots, x_N\right)$ and calculating the function value corresponding to each random sample $H\left(x_i\right)$. Finally, the mean $\hat{L}$ of these is used as an unbiased estimate of the value L of the quantity to be sought, i.e., there is:

$$\hat{L} = \hat{E}(H) = \frac{1}{N} \sum_{i=1}^{N} H\left(x_i\right) \tag{9}$$

$\hat{L}$ The estimation error of the quantity to be sought L is determined by its variance:

$$Var(\hat{L}) = E\left(\frac{1}{N} \sum_{i=1}^{N} \left[H\left(x_i\right) - L\right]\right)^2 = \frac{1}{N} Var(H(x)) \tag{10}$$

The sampling calculation accuracy is usually expressed in terms of the coefficient of variance β, which is calculated as shown in the following formula:

$$\beta = \frac{\sqrt{Var(\hat{L})}}{\hat{L}} = \frac{\sqrt{Var[H(x)]/N}}{\hat{L}} \tag{11}$$

The smaller β means the better the calculation accuracy. From the above equation, the relationship between the number of samples to be taken and the computational accuracy as well as the amount to be estimated is obtained as:

$$N = \frac{Var[H(x)]}{(\beta \hat{L})^2} \tag{12}$$

The formula shows that when the sample variance is certain, the number of required samples is inversely proportional to the product of computational precision and the amount to be estimated. It shows that the higher the precision requirement, the smaller the to-be-estimated L, the more the number of samples required, and the more difficult the sampling estimation work, which is the difficulty of the Monte Carlo method for the probabilistic simulation of rare events.

Monte Carlo methods are also known as statistical test methods or random sampling techniques. Monte Carlo can be used to solve multi-dimensional problems. The reliability assessment of distribution networks using Monte Carlo simulation is categorized into sequential simulation algorithms, non-sequential simulation algorithms, and pseudo-sequential simulation algorithms, depending on whether or not the temporal sequence of system states is considered.

The sequential simulation algorithm can accurately simulate the duration of the system in each state and the transition frequency between states. Therefore, this algorithm can not only obtain the reliability index of each load in the distribution network, but also obtain the time sequence information of the system operating state, and can accurately calculate the frequency and duration index of reliability. In the system containing distributed generation, such as solar power generation, wind power generation, etc., the sequential Monte Carlo method can establish a more realistic probability model, which can well assess the reliability indexes of the distribution network under the influence of time, season, weather and other factors, and the credibility of the calculation results is high.

The reliability assessment algorithm using sequential simulation can accurately calculate the annual average number of component failures and the probability distribution statistics of annual failure time while obtaining probability indicators and expected value indicators. However, the sequential simulation algorithm also has certain shortcomings, due to the need to store all the components of the reliability state sequence and its duration, resulting in a very serious memory occupation of the computer.

The non-sequential simulation algorithm is a non-real-time simulation method. This algorithm has the advantages of simple model, low memory requirement, and significantly better convergence speed than the sequential simulation algorithm, which is suitable for large-scale power system evaluation calculations as well as occasions with higher requirements for calculation speed. However, because the method is difficult to calculate the frequency and duration indicators of power system reliability, the data information obtained is not rich enough to meet the engineering needs.

3.3.2. Monte Carlo method simulation modeling. The main method used in this paper is the sequential Monte Carlo method. In the study, it is assumed that the failure rate of the component is in a stable and constant operating period, i.e., the failure rate of the component is constant. At this time, the operating curve of the component is obeying an exponential distribution. Based on this assumption, the failure-free operating time TTF of the component is obeying a negative exponential distribution, i.e., TTF has probability density $f(t)$:

$$f(t)=\begin{cases}\lambda e^{-\lambda t} & t\geq 0\\ 0 & t\leq 0\end{cases} \tag{13}$$

Can be obtained from the above equation:

$$T_w=-\ln\delta/\lambda \tag{14}$$

$$T_r=-\ln\delta/\mu \tag{15}$$

After sampling according to the above 2 formulas, the sequence of operating states of each component in a certain simulation time can be obtained.

1) Calculation method of reliability index. According to the formula of reliability indicators, the reliability assessment of load points using the Monte Carlo method is mainly to calculate their annual failure outage rate λ (times/year), annual average outage duration U (hours/year), average outage duration r (hours/times), and the total load electricity underconsumption expectancy EENS (kilowatt-hours/year). The specific calculations for these reliability metrics are described below:

$$\lambda_j=\frac{N_j}{\sum T_{uj}} \tag{16}$$

$$r_j = \frac{\sum T_{dj}}{N_j} \tag{17}$$

$$U_j = \frac{\sum T_{dj}}{\sum T_{dj} + \sum T_{uj}} \tag{18}$$

$$EENS_j = P_{average} \times U_j \tag{19}$$

where, λ_j is the failure outage rate of the load numbered j, T_s is the normal operating time of the load point during a particular simulation run, T_d is the repair time of the load point during a particular simulation run, i.e., the time to failure, N_j is the total number of load failures throughout the simulation years, and $P_{average}$ is the average power of the load.

2) Calculation of reliability failure probability distribution. Assuming that parameter k is the number of failures of the load per year during the Monte Carlo simulation, and $m(k)$ is the statistics of the number of different outages of the load point in a year, the probability distribution of outages of the load point throughout the simulation $p(k)$ can be calculated as:

$$p(k) = \frac{m(k)}{M} k = 0,1,2\cdots\cdots \tag{20}$$

where M is the total number of simulation years.

The method of calculating the probability distribution of outage time at a load point due to a fault is similar to the above. Assume i is the interval of outage time for the load for each year of the simulation, and $n(i)$ is the outage time statistic for that load point over the course of the year. Because outage time is an uncertain quantity, the pattern of outage time can be better seen by using interval statistics. Generally, the pattern is counted in intervals of hours, then the probability distribution of outage time at the load point $p(i)$ can be calculated as:

$$p(i) = \frac{n(i)}{M} i = 0 \sim 1, 1 \sim 2, 2 \sim 3\cdots\cdots \tag{21}$$

3) Random number generation method. The generation of random numbers is a key issue in the Monte Carlo method. The random number r sampling formula is:

$$\begin{aligned} x_i &= \left(2053 x_{i-1} + 13849\right)\left(\bmod 2^{16}\right) \\ r_i &= x_i / 2^{16}, i = 1,2,\ldots\ldots \end{aligned} \tag{22}$$

Eq. When $i > 2^{16}$, the random number restarts the cycle.

The generation of random numbers using a computer begins with the generation of a base time, which uses the system time for its initial value, i.e., $x_0 = time(0)$. Next, the random number generated in the previous generation is used as the seed for the next generation of random numbers, which is transformed into a variable similar to the system time, x_i:

$$x_i = \frac{(j+1.02)}{(j+1.01)} \times x_{i-1} \times r_{i-1} \tag{23}$$

where, j is the number of times the simulation is cumulative, and when $j > 50$, the seed is corrected once by making $j > 1$ and $x_i = \sqrt{x_{i-1} \cdot x_0}$. The seeds are then used to generate random numbers using the method of multiplication with remainder. Since the seed is different each time, thus the random number obtained is different.

3.3.3. Flow of the Monte Carlo assessment methodology. The process of applying Monte Carlo methods to analyze power system reliability indicators can be roughly divided into three steps: system state sampling, system state analysis and system indicator statistics.

Pseudo-sequential simulation adds the process of system analysis and evaluation in the random state sampling stage. If the state obtained from sampling is the fault state of load cutting, then the sequential simulation algorithm is used to obtain the time sequence information of the outage, otherwise the sampling continues. The pseudo sequential simulation algorithm flow is shown in Fig. 2.

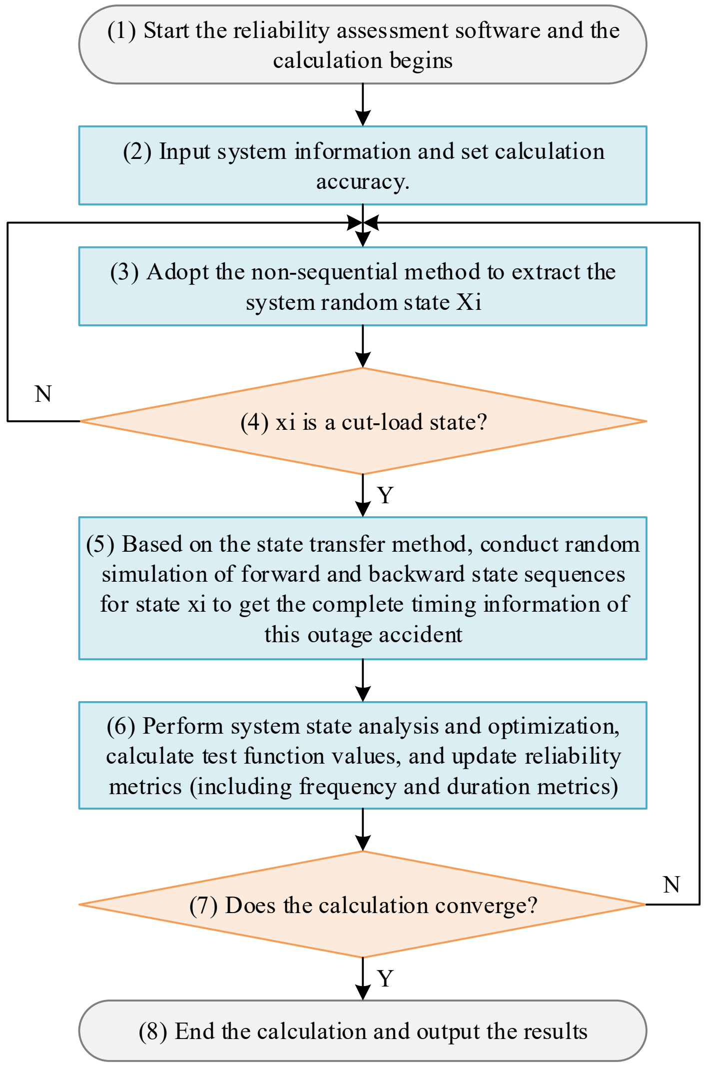

Fig. 2. Pseudo-sequential simulation algorithm process

4. Performance assessment of new energy distribution systems

4.1. Self-healing of faults in new energy distribution networks

Self-healing is an important feature of smart distribution grids and an important symbol of completion. Self-healing of distribution network refers to continuous online self-assessment of the operational status of the grid, and the use of preventive control means, timely detection, rapid diagnosis and elimination of hidden faults. When a fault occurs, it can quickly isolate the fault and recover itself without or with a small amount of human intervention, avoiding the occurrence of large-scale power outages.

Distribution network fault self-healing covers many new technologies in the fields of automatic control, relay protection, computer and software technology, applied mathematics, etc. It is a comprehensive control technology that integrates software and intelligent hardware devices. It requires the distribution system to have the following hardware and software conditions. ① Strong and flexible distribution network architecture (such as ring network or hand in hand power supply network, etc.), the existence of multiple power supply path. ② Distributed and coordinated intelligent devices and equipment (such as data acquisition devices, telecontrol devices, etc.), which can monitor and operate the entire network. ③ Standard and integrated intelligent dispatch center. ④ Advanced visualization monitoring and fast simulation software based on self-healing theory.

The distribution system generally has multiple power supply paths and its network structure can be flexibly changed, which is the basis for realizing the self-healing of faults in the distribution network. With various intelligent switches and distribution terminal equipment. Reliable communication network. Automated processing software system.

4.1.1. Framework system for self-healing control. Nowadays, the most commonly used architecture system in distribution network is “2-3-6” architecture, which is the basic organization structure for distribution network self-healing to realize distribution autonomy, wide-area coordination, and adaptability to working conditions, and consists of two loops of control logic, three layers of control structure, and six control links that are closely connected to each other.

1) Two-loop control logic

2) Three-layer control structure: the 3-layer control structure includes a high-end decision-making layer, an intermediate coordination layer and a local reaction layer.

3) Six control links: Along the direction of information flow, there are six control links on the three-layer control structure: acquisition and measurement, monitoring and coordination, working condition evaluation, control program, deployment coordination and control action.

4.1.2. Distribution network fault identification and protection coordination:

1) Obtain the voltage at the fault point. In order to ensure that the line fault occurs when the two ends of the four remote control volume can be achieved double communication without line length, usually set the main protection of distribution network line protection for fiber optic differential protection, which makes the whole length of the line can be protected, and with the rapid development of fiber-optic information technology, electrical four remote volume of the two sides of the collection of the measurement results can be more accurately reflect the fault in the whole line in the location of the failure to enhance the location of faults. Localization.

The voltage calculation of transition resistance is shown by Eq:

$$\dot{U}_{An} = \dot{U}_{Rf} + \alpha U_{xL} \tag{24}$$

$$\dot{U}_{An} = \dot{U}_{Rf} - (1-\alpha) U_{xL} \tag{25}$$

The distance from the point of failure to m is expressed by setting a to 1' than the total length of the whole line I.

Equations (24) and (25) can be deduced from equation (26):

$$U_{AL} = \dot{U}_{Am} - \dot{U}_{An} \tag{26}$$

The fault point voltage can be solved by the following equation:

$$\dot{U}_{Rf} = (1-\alpha)\dot{U}_{Am} + \alpha \dot{U}_{An} \tag{27}$$

In the case of instantaneous faults, the line cuts off the industrial frequency operating voltage on both sides of the phase, which can be expressed as:

$$\dot{U}_{Am} = \dot{U}_y + \frac{1}{2}\dot{U}_{xL} \quad (28)$$

$$\dot{U}_{An} = \dot{U}_y - \frac{1}{2}\dot{U}_{xL} \quad (29)$$

$$\dot{U}_{Am} - \dot{U}_{An} = \dot{U}_{xL} \quad (30)$$

Then the voltage at the point of fault is:

$$\dot{U}_f = (1-\alpha)\dot{U}_{Am} + \alpha\dot{U}_{An} \quad (31)$$

2) Method of determining and handling transient and permanent faults. In determining the type of fault, the most serious consequences that may be caused by a permanent fault should be taken as the criterion for setting the voltage criterion, so the voltage setting value can be determined according to the following arithmetic equation:

$$U_{Dz} = kU_{AL} \quad (32)$$

Setting U_{Dz} is the voltage determination value, U_{xL} is the electromagnetic coupling voltage in which the fault occurs causing the missing operation state and is at the maximum load, where the coefficient k is taken as 1.1 to 1.2.

It can be seen that when U_{Dz} is less than the actual monitored voltage when the fault occurs, the reclosing gate can be acted on to identify the fault as a transient fault, and vice versa for permanent faults, the reclosing gate is not acted on.

In the line no-load operation with the fault phase voltage on both sides of the completion of the determination of the relationship. Namely:

$$U_y \geq kU_{Al} \quad (33)$$

The length of the applicable line is calculated as:

$$1 \leq \frac{U_y}{kU_x} \quad (34)$$

From the above formula can be deduced, suitable for the determination of the line length will be affected by the size of the load, when the greater the current-carrying line length can be determined the shorter the line length, and vice versa, if the line is unloaded, the line length can be determined for the maximum length.

Convenient to analyze, first assume $U_y / U_{xL} = m$, then the end voltage at both ends of the line in the faulty phase is:

$$\left|\dot{U}_{An}\right| = \left|\dot{U}_{An}\right| = \sqrt{U_y^2 + \left(\frac{U_{xL}}{2}\right)^2} = U_{xL}\sqrt{m^2 + \frac{1}{4}} \quad (35)$$

When $0 \leq m \leq \sqrt{3}/2$ is $\left|\dot{U}_{Am}\right| = \left|\dot{U}_{An}\right| < U_{xL}$, this time the instantaneous fault will be misclassified as a permanent fault by the voltage determination method.

If the fault on the line is a permanent earth fault, the distance from the point of contact to the tripped circuit breaker will be proportional to the voltage on both sides of the faulted phase. Therefore, to achieve the best results in determining the length of the line, this criterion needs to be compensated on both sides of the line $U_{xL}/2$. Equation (36) is a criterion for determining whether the fault category is an instantaneous fault (initiating the reclosing action), and it is important to note that this is based on the principle that the direction of the busbar current is the positive direction. That is:

$$\left|\dot{u}-\frac{\dot{U}_{AL}}{2}\right|\geq\left|\frac{k\dot{U}_{xL}}{2}\right| \tag{36}$$

where $\dot{U}$ is the measured voltage of the faulted disconnected phase.

According to the above arithmetic equation, it can be seen that when the fault is transient, the electromagnetic coupling voltage and the capacitive coupling voltage will simultaneously affect the voltage at both ends of the faulted disconnected phase. When the fault is permanent, the voltage at both ends of the faulted line will not exceed $U_{xL}/2$.

Equation (37) shows the calculation based on the compensation voltage as the determination condition of reclosing action:

$$U_y\geq\frac{kU_{AL}}{2}=\frac{k}{2}U_xI \tag{37}$$

This leads to the applicable length of the compensation voltage criterion:

$$1\leq\frac{2}{k}\cdot\frac{U_y}{U_x} \tag{38}$$

Comparing the two equations, the applicable line distance of the working voltage judgment basis is only half of the line distance satisfied by the compensating working voltage judgment basis. Therefore, the compensation voltage judgment basis can improve the actual line distance is shorter, the voltage amount of judgment brought about by the error problem.

Combined voltage compensation judgment basis of analysis, is to solve the long distance high voltage line installed shunt reactor. And the neutral point is also equipped with reactor, the line occurs instantaneous fault, fault disconnection phase voltage, after the circuit breaker action will fall to a very low value of the problem. To wit:

$$\left|\dot{U}-\dot{U}_{XL}/4\right|\geq\left|k\dot{U}_{AL}/4\right| \tag{39}$$

$$\left|\dot{U}-3\dot{U}_{XL}/4\right|\geq\left|k\dot{U}_{AL}/4\right| \tag{40}$$

Combined voltage compensation after the occurrence of the fault determination results simultaneously meet (39), (40), it can be determined that the fault is permanent, combined compensation voltage determination method of the line applicable length calculation. Similarly compensated voltage determination method and similar to the above two categories of judgment based on similar, leading to misjudgment results of the most direct factors, the permanent short circuit fault fault point is closer to the port distance, it is more likely to cause calculation errors. However, in the instantaneous faults are more able to meet the quasi-request to identify faults, because the combination of compensation judgment method because the new power angle is smaller, the possibility of misjudgment is also smaller.

4.2. Analysis of distribution network construction

The scope of the construction area in this paper covers an area of about 15 square kilometers, with a total power supply population of about 160,000 people. The construction area is the core area of the city. This area has a concentrated population, huge potential for power supply, high requirements for power supply reliability, and is a newly built urban area, which is also easy for the construction of distribution network automation engineering.

The power supply distribution in the region has been basically completed and the network structure has stabilized. Since 2013, the annual maximum load growth rate of the construction area has reached 21%. Currently, the load in the area has reached 110 MW, with an average load density of 10.21 MW/km^2. The power line corridors in the area have basically stabilized, and most of the lines have undergone pole and line undergrounding or relocation works, and have been put into operation for no more than 10 years.

Currently there are a total of 3 substations supplying power to the construction area, namely: Wangjiaping 220 kV substation, Zhangjiajia 110 kV substation, Lianhua 110 kV substation, and 25 10 kV lines supplied. Among them, 10 Zhangjia transformers, 13 Lotus transformers and 2 Wangjiaping transformers.In 2016, CityNet will build 3 new 10kV lines within the construction.

Wangjiaping 220kV substation and Zhangjiajia 110kV substation and Lotus 110kV substation supplying power to the construction area are all dual power supply sources with two or more main transformers and self-transfer devices, which make the power supply highly reliable and safe.

There are 32 10kV power supply lines in the construction area, with a total length of 196.4km. 25 of the 32 10kV lines are interconnected, with an interconnection rate of 78%, and the average load of the distribution lines is 5.01MW/line.

4.2.1. Self-healing system data communication program design. According to the requirements of the self-healing system for data communication and the current situation and construction objectives of the distribution network discussed in this paper, the data communication system of the self-healing control system of the distribution network is designed as follows:

1) The electric power communication network can be divided into electric power communication backbone network and electric power communication access network in terms of its level. The power communication access network adopts passive optical network technology and medium-voltage power broadband carrier technology. The transmission network adopts SDH network, and the fiber optic access network is connected to the SDH backbone network through the dispatching data network. In addition, it has reconstructed and expanded the main station of the Municipal Bureau and 220kV Wangjiaping Transformer, 110kV Lotus Transformer, 110kV Zhangjiayuan Transformer, 110kV Seven Districts Transformer, 110kV Yodangchong Transformer, 110kV Pine Transformer, and built a dedicated network for distribution communication on the backbone of the city's optical ring network.

2) Interface mode. The main interfaces of the optical fiber private network communication mode are as follows:

Interface between OLT and backbone SDH optical transmission equipment: FE interface.

Interface between ONU and distribution terminal: FE interface.

The main interfaces of the medium-voltage power broadband carrier communication mode are as follows:

Interface between the medium-voltage power broadband carrier bridge (headend) and the EPON terminal ONU: FE interface.

Interface between the medium voltage power broadband carrier bridge (headend/terminal) and the inductive coupler: signal coupling port.

Interface between the medium-voltage power broadband carrier bridge (terminal) and the distribution terminal: FE interface.

4.2.2. Self-healing system data communications program implementation. Combined with the construction of this distribution automation project, the EPON distribution communication system involves a total of 27 lines in 6 substation sub-stations, including the main station of Zhuzhou Bureau, Wangjiaping, Zhangjiajia, the seven districts, Pine, Yautangchong and Lianhua.

1) EPON each network layer equipment selection and configuration are as follows: Optical Line Terminal (OLT): 1 OLT device is set up in each of the 6 stations, such as Wangjiaping Station, Zhangjiazui Station, Seven Districts Substation, Pine Tree Substation, Yautangchong, Lotus Substation, and so on.

Optical Distribution Network Terminal (ODN): According to the geographic location of each 10kV distribution network terminal, it is considered to centrally set up one level of optical distributor in the substation, and the ratio of optical distribution is considered to be 1:4 uniform optical distribution.

Optical network terminal (ONU): ONU is deployed according to the DTU/FTU setting of distribution terminal.

2) The network elements are set as follows: Combined with the distribution terminal of 10kV line and optical cable laying in the distribution network of this distribution automation construction area, this project sets OLT1 sets in each of the six substations, including Wang Jiaping Substation, Zhangjiajia Substation, Seven Districts Substation, Pine Substation, Mithangchong Substation, Lotus Substation, and so on.

4.3. New energy system simulation experiment

The arithmetic examples in this paper are done on a personal computer equipped with an AMD Ryzen 9 3900X CPU (3.8GHz/12 cores and 24 threads) and 64GB of RAM.

Based on MATLAB and GUROBI platforms, this paper utilizes an integrated electricity-gas-heat coupled district energy system including a 35-node distribution grid, a 15-node gas distribution network and a 38-node heat distribution network as a case study. The new energy distribution grid system reliability assessment method proposed in this paper is simulated and validated.

The reliability parameters of the new energy distribution grid system are shown in Table 1, and the failure rate of each component is less than or equal to 0.7. Based on the Indoor Air Quality Standard, the heating indoor temperature is set to be 16-24°C and the external environment is set to be -10°C. And it is assumed that the current heating indoor temperature is 24°C.

Table 1. Reliability parameters of the new energy distribution system

Serial number	Element type	Inefficiency (failure times per year)	Fault repair (h)
1	Mesh line	-	6.2
2	Pneumatic channel	0.3500	21.3
3	Heat network pipeline	0.7000	50.4
4	Wind power unit	0.4012	21.5
5	Electric cooker	0.036	200.4
6	CHP unit	0.034	300.6
7	Combustion chamber	0.0055	20.4
8	Gas turbine	0.0055	300.8
9	Waste heat boiler	0.0045	300.4
10	Steam turbine	0.0085	300.9

4.3.1. Reliability modeling analysis of coupled components. From the hybrid energy router (CHP) unit structure and CHP unit states, a Markov state transfer matrix is generated. The transfer probabilities between each CHP unit state are counted, and the four-state reliability model of the CHP unit, which are normal operation, reduced power and heat supply, reduced power supply, and system shutdown. Based on the Markov chain resolution method to calculate the probability and average duration of each operating state, the reliability index of CHP unit is shown in Table 2.

Compared with the traditional two-state model (normal operation, system shutdown), the outage probability of the CHP unit in the (reduced power and heat supply, reduced power supply) state model is reduced by 50%. The average outage durations of heat supply and power supply are 257h and 206h, respectively, which are reduced by 27.06% and 13.64%, effectively improving the accuracy of coupled equipment reliability modeling.

Table 2. CHP unit reliability index

Type	Running state	State probability	State frequency f /time/year	Mean duration d /year
1	Normal operation	0.9991	0.0253	33.645
2	Electric heating	2.3014×10^{-4}	0.0065	0.0308
3	Reduced power supply	2.6359×10^{-4}	0.0055	0.524
4	System shutdown	2.7781×10^{-4}	0.0125	0.0937

4.3.2. Reliability indicator assessment results. Utilizing Monte Carlo methods can evaluate system metrics in addition to load metrics. The system reliability metrics for the test network in this paper are shown in Table 3.

Table 3. This paper tests the system reliability index of the network

The average power outage frequency of the system. SAIFI (fr/syst.cust)	1.023321
The average outage duration of the system. SAIDI (hr/syst.cust)	25.634564
The average user's average power outage lasts. CAIDI (hr/cust)	23.7127933
Average power availability index. ASAI	0.983364
Average power supply unavailability index. ASUI	0.003516
Total power failure. EENS (MWh/yr)	282.131364
The average user power outage. AENS (MWh/yr/syst.cust)	0.096778

For the impact of different system structures on the reliability of new energy distribution networks, this paper carries out calculations on the following scenarios and compares the calculation results. The simulation period is 1500 years.

The results of the new energy distribution network reliability indicators are shown in Table 4.

Case 1: No fuse protection, no counting of planned maintenance, no counting of switch refusal, no counting of standby.

Case 2: With fuse protection, without counting and planned maintenance, counting and switch refusal, counting and standby.

Case 3: with fuse protection, counting and planned maintenance, counting and switch refusal, counting and standby.

In the case of new energy distribution network without fuse and standby transformer, the average outage frequency of the system reaches 1.045281, while in the case of standby transformer and fuse protection, the SAIFI can be reduced to 1.005344, and the average power supply availability index can reach more than 0.99. It can be concluded that the reliability of the distribution network can be improved if fuses and standby transformers are introduced in the distribution network.

Case 3 shows the reliability index of the new energy distribution network when considering planned maintenance. In this paper, on the basis of the original reliability index of distribution network, the reliability index of planned maintenance is accumulated. Planned maintenance is helpful for the improvement of distribution network reliability. It is not possible to analyze the impact of planned maintenance on reliability from the point of view of data alone, but the reduction of component failure rate by planned maintenance should be considered comprehensively. And further analyze its impact on distribution network.

Table 4. Evaluation of reliability index of new energy distribution network

Evaluation index	SAIFI	SAIDI	CAIDI	ASAI
Case 1	1.036551	25.332114	23.501246	0.995634
Case 2	1.005344	6.9215323	6.7425543	0.996071
Case 3	8.364937	35.416786	6.8522736	0.998609

4.3.3. Reliability assessment analysis of new energy systems. According to the assessment process, the sequential Monte Carlo method was used for reliability assessment. When the simulation proceeded to 300 years, the variance coefficient was lower than 0.1 and the simulation converged. In this process, a total of 50,134 failure scenarios were sampled, accounting for 0.317%. There were 49,251 first-order faults and 883 second-order faults. The number of faults in the electric, gas, and heat networks were 721, 12004, and 35177, respectively. In the fault-free operation simulation, the simulation time for a single section is 4.54s, while the fault simulation time for the single fault consequence analysis is 43.71s.

After simulation calculation, the results of the reliability index of new energy distribution network system are shown in Table 5. In the new energy system, among all kinds of subsystems, the total load of the gas network is 16.5674 MW. It is in higher demand compared to the grid and the heat network. Therefore, although the LOLP indicator for the gas grid is much lower than the grid, the EENS indicator is the highest. Meanwhile, the SAIFI and SAIDI indicators for the heat grid are much lower compared to the gas grid due to the fact that the heat grid has more users than the gas grid.

Table 5. Reliability of the new energy distribution system

Index	Electricity	Gas	Heat	New energy distribution system
LOLP	1.8644×10^{-6}	1.6684×10^{-2}	2.3659×10^{-2}	3.6004×10^{-2}
EENS	1.3367×10^{-1}	5.1118×10^{2}	2.0015×10^{2}	7.2077×10^{2}
SAIFI	6.0439×10^{-8}	1.7931×10^{-3}	8.7261×10^{-4}	4.5865×10^{-4}
SAIDI	4.5507×10^{-3}	5.6931	7.1124	9.8364

The impact of multi-state modeling of components is analyzed on the basis of the known system reliability by comparing the reliability of the CHP unit under the four-state model with the two-state model for an integrated regional energy system. In this case, P1 and P2 represent the loss-of-load probabilities under the two-state model and the multi-state model, respectively, while E1 and E2 represent the loss-of-load expectations, respectively. The comparison of reliability metrics under the two CHP reliability models is shown in Table 6.

The loss of load probability and expected loss of load of the new energy distribution system under the four-state model of the cogeneration unit is lower, mainly because the unit's states of “reduced power and heat supply” and “reduced power supply” are taken into consideration, taking into account the fact that when the turbine, the waste heat boiler and other components fail, the system will continue to ensure the supply of electricity and heat by adjusting the operation mode of the unit, and will be able to provide the electricity and heat supply through the adjustment of the operation mode. The reliability assessment is therefore closer to the actual scenario. Therefore, the reliability assessment is closer to the actual scenario and the results are more accurate.

Table 6. Two types of CHP reliability models are compared

System	$P1(p.u)$	$P2(p.u)$	$E1(MW\cdot h/a)$	$E2(MW\cdot h/a)$
Electricity	3.2654×10^{-6}	2.3315×10^{-6}	2.6539×10^{-1}	1.7534×10^{-1}
Gas	1.5693×10^{-2}	1.5486×10^{-2}	5.1147×10^{2}	5.7866×10^{2}
Heat	3.5269×10^{-2}	2.3659×10^{-2}	2.9995×10^{2}	2.2358×10^{2}
New energy distribution system	4.7947×10^{-2}	3.5784×10^{-2}	7.9964×10^{3}	7.0039×10^{2}

The influencing factors that cause the difference in the reliability of each subsystem are further analyzed by comparing the average failure rate of pipelines/lines in the network (S_1), the average failure repair time (S_2), the number of pipelines/lines (S_3), the structure of the network (S_4), and the types of failure recovery measures (S_5). The comparative analysis of electricity, gas and heat systems in the new energy distribution network system is shown in Table 7.

Despite the low failure rate of heat network pipelines, their radial, non-redundant nature results in a single failure recovery measure and long recovery time, which leads to the highest probability of heat network loss of load at 0.02355.

In the event of a fault, fault recovery measures include the use of distributed power sources, multi-energy complementary systems, and thermal inertia and other means to form an island or delay the loss caused by the fault. These measures are effective in securing power supply to distribution network loads, thereby improving power supply reliability. Therefore, reducing the failure rate of gas and heat network pipelines, shortening the time to repair failures, and increasing the number of standby pipelines can help improve the reliability of the entire system.

Table 7. The new energy system is compared to the electric, gas and thermal system

System	S_1	S_2	S_3	S_4	S_5
Electricity	0.0124	6h	40 piece	Redundancy	Multiple
Gas	0.1508	21h	16 piece	Partial redundancy	Single
Heat	0.0932	53h	28 piece	Single	Single

4.4. *Distribution network self-healing system testing*

RTDS is a device specialized in the study of electromagnetic transient phenomena in power systems, in which an active distribution network model can be easily constructed using the accompanying simulation software. Utilizing the rich input and output interfaces of RTDS, RTDS can be easily interacted with external physical devices. Therefore, RTDS can be used to test the developed smart terminal unit (STU) device for distribution networks and the self-healing system it consists of.

4.4.1. Test basis:

1) Simulation Model. Due to the limitation of the number of devices and the number of power amplifier analog amplification, the test cannot use a very complex simulation model. The active distribution network primary system wiring built in RTDS.

The relevant parameters of the simulation system are shown in Table 8. Since the simulation models of motor-type DGs and inverter-type DGs are built separately, then they can be replaced as needed during simulation.

Table 8. An active distribution network is a system parameter

Element	Project	Parameter
System power 1	Voltage	10kV
	Impedance	$1\angle 80°\,\Omega$
	Capacity	∞
System power 2	Voltage	10kV
	Impedance	$1\angle 80°\,\Omega$
	Available allowance	6MW
System power 3	Voltage	10kV
	Impedance	$1\angle 80°\,\Omega$
	Available allowance	12MW
Line	Length	0.23km
	Positive sequence impedance	$(0.23+0.36\,j)\,\Omega/km$
	Zero sequence impedance	$(0.45+16\,j)\,\Omega/km$
DG1	Type	Motor class
	Capacity	5MW
DG2	Type	Contravariant
	Capacity	5MW
L1-L5	Power	5MW

2) Instruments under test. The instruments under test are the five STUs developed, which are two units at the common feeder node, one unit at the DG node, and two units at the contact switch. Due to the limited number of devices under test, the devices at the DG node will be tested separately according to the DG being a type A DG and a type B DG.

3) Closed-loop system construction. In order to utilize the RTDS system to test the STU, it is necessary to establish a closed-loop test system between the two. The basic construction method is to build an active distribution network simulation model in the RTDS system. After successfully running the model, the GTAO board of RSCAD is used to output the corresponding analog data in the model. The analog signal generated by RTDS is amplified by an amplifier and connected to the corresponding STU, so that the STU acquires voltage and current signals to simulate the scene of connecting to the actual distribution network.

4.4.2. Fault localization and isolation. Using the active distribution network closed-loop test platform built in this chapter, the STU device can be tested in closed-loop, and this section first tests the ability of the STU to realize distributed fault segment localization and isolation.

When there is no DG downstream of a fault point, the fault current characteristics at this time are similar to those of a traditional passive distribution network, with short-circuit currents flowing at both ends of the faulted section only on the near-supply side, and the scheme proposed in this paper should also be able to adapt to such a fault situation.

The recorded waveforms after a metallic three-phase transient fault occurs at place f_3 are shown in Fig. 3. K25 and K45 represent the opening and closing states of the corresponding circuit breakers. If the fault occurs at f_3 in the figure and there is no power supply to provide short-circuit current downstream of the fault point, the test results of fault section localization and isolation are as follows.

From the figure, it can be seen that about 66ms after the fault occurs, STU3 sends a signal to jump open K25. Since there is no fault current flowing through STU4, STU4 is remotely controlled by STU3 to jump open K45. After a delay (set to 530ms), K25 closes, and since the fault has disappeared, K25 closes successfully, and STU3 then informs STU4 to make K45 close, restoring the original system power supply.

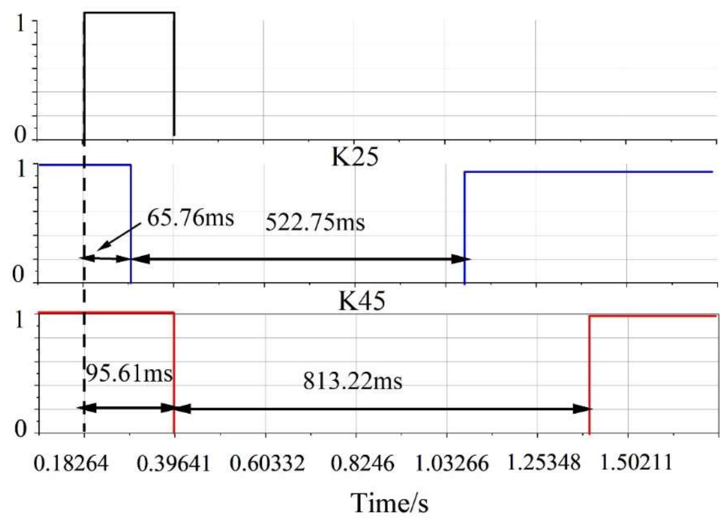

Fig. 3. After the transient failure

When the short-circuit current that can be supplied by the DG is high, the far power side STU can be activated and is able to act autonomously to remove the fault. Other than this, the remote power supply side switch needs to be remotely disconnected by the near power supply side STU. Simulation tests are carried out for three-phase short circuits and two-phase short circuits with different transition resistances (0Ω, 2Ω, 5Ω, 10Ω, 15Ω) at locations f_2 and f_3, respectively, and the switches on both sides of the faulted section are able to operate correctly. In order to obtain the action time parameter of the switch, each test is carried out 10 times, and the action time of the relevant switch is shown in Table 9. Since the reclosing time parameter can be set artificially, it will not be analyzed specifically.

Regardless of whether a DG exists downstream of the faulted section or not, and regardless of whether the short-circuit current provided by the DG can cause the local STU to activate, the average fault removal time does not exceed 95 ms, and the STUs at both ends of the faulted section can accurately act to remove the fault. The distribution network fault self-healing system is capable of rapid fault localization and fault treatment.

Table 9. Fault section location and isolation time

Fault type	Dg can make the remote power side	STU booting	Dg cannot make the remote power side	STU booting
Switch	Near power side	Remote side	Near power side	Remote side
Minimum failure time(ms)	59.63	62.04	59.67	89.65
Maximum failure time(ms)	67.22	69.75	66.43	95.21
Mean fault removal time(ms)	65.46	65.31	63.79	94.17

5. Conclusion

This paper utilizes the sequential Monte Carlo method to assess the reliability of new energy distribution network system. A self-healing control framework system and a data communication scheme are designed for the distribution network, and a simulation environment is constructed to test the fault localization and isolation processing of the new energy distribution network.

Calculate the reliability indexes of CHP units in four states (normal operation, heat reduction, power reduction, and system shutdown) using the Markov chain analysis method. The heat supply and power supply of the new energy distribution network are reduced by more than 10% under the states of reduced heat supply and reduced power supply units, which effectively improves the accuracy of the reliability modeling of the coupled equipment. The average power supply availability index of the new energy distribution network system can reach over 0.99 under the conditions of fuse protection, counting and planned maintenance, counting and switching refusal action, counting and standby. A new energy distribution network closed-loop test platform was constructed, and the developed STU was tested in closed-loop simulation using this platform. The distribution network fault self-healing data scheme is able to locate and process faults within 95ms and carry out fault isolation, eliminating faults to realize fault self-healing.

Funding

Research and Demonstration Project on Adaptive Whole-domain Distribution Network Self-healing Technology Considering Distributed Resource Carrying Capacity Across Multiple Time Scales - Topic 1: Constructing a Model for Evaluating Self-healing Failures and Fault Analysis Based on Multi-dimensional Data Variables and Intelligent Algorithms(GZKJXM20222422).

References

[1] Pan, E., Liu, S., Liu, J., Qi, Q., & Guo, Z. (2020). The state grid corporation of China's practice and outlook for promoting new energy development. Energy Conversion and Economics, 1(2), 71-80.

[2] Paithankar, Y. G., & Bhide, S. R. (2022). Fundamentals of power system protection. PHI Learning Pvt. Ltd..

[3] Kong, X., Xu, X., Yan, Z., Chen, S., Yang, H., & Han, D. (2018). Deep learning hybrid method for islanding detection in distributed generation. Applied Energy, 210, 776-785.

[4] Kim, M. S., Haider, R., Cho, G. J., Kim, C. H., Won, C. Y., & Chai, J. S. (2019). Comprehensive review of islanding detection methods for distributed generation systems. Energies, 12(5), 837.

[5] Ibrahim, A. H. M., Sadanandan, S. K., Ghaoud, T., Rajkumar, V. S., & Sharma, M. (2024). Incipient Fault Detection in Power Distribution Networks: Review, Analysis, Challenges and Future Directions. IEEE Access.

[6] Azeroual, M., Boujoudar, Y., Bhagat, K., El Iysaouy, L., Aljarbouh, A., Knyazkov, A., ... & Markhi, H. E. (2022). Fault location and detection techniques in power distribution systems with distributed generation: Kenitra City (Morocco) as a case study. Electric Power Systems Research, 209, 108026.

[7] Arefifar, S. A., Alam, M. S., & Hamadi, A. (2023). A review on self-healing in modern power distribution systems. Journal of Modern Power Systems and Clean Energy, 11(6), 1719-1733.

[8] Mirshekali, H., Dashti, R., Keshavarz, A., Torabi, A. J., & Shaker, H. R. (2020). A novel fault location methodology for smart distribution networks. IEEE Transactions on smart grid, 12(2), 1277-1288.

[9] Dashtdar, M., Dashti, R., & Shaker, H. R. (2018, May). Distribution network fault section identification and fault location using artificial neural network. In 2018 5th international conference on electrical and electronic engineering (ICEEE) (pp. 273-278). IEEE.

[10] Alcala-Gonzalez, D., García del Toro, E. M., Más-López, M. I., & Pindado, S. (2021). Effect of distributed photovoltaic generation on short-circuit currents and fault detection in distribution networks: A practical case study. Applied Sciences, 11(1), 405.

[11] Garau, M., Ghiani, E., Celli, G., Pilo, F., & Corti, S. (2018). Co-simulation of smart distribution network fault management and reconfiguration with lte communication. Energies, 11(6), 1332.

[12] Campos, R. M., Figueroa, C. C., Oyarzún, H. V., & Baeza, J. M. (2018, May). Self-healing of electric distribution networks: A review. In 2018 7th International Conference on Computers Communications and Control (ICCCC) (pp. 63-70). IEEE.

[13] Refaat, S. S., Mohamed, A., & Kakosimos, P. (2018, April). Self-Healing control strategy; Challenges and opportunities for distribution systems in smart grid. In 2018 IEEE 12th International conference on compatibility, power electronics and power engineering (CPE-POWERENG 2018) (pp. 1-6). IEEE.

[14] Shirazi, E., & Jadid, S. (2019). A multiagent design for self-healing in electric power distribution systems. Electric Power Systems Research, 171, 230-239.

[15] Nikolić, J., Jubatyrov, N., & Pournaras, E. (2021). Self-healing dilemmas in distributed systems: Fault correction vs. fault tolerance. IEEE Transactions on Network and Service Management, 18(3), 2728-2741.

[16] Shen, Y., Chen, Y., Zhang, J., Sang, Z., & Zhou, Q. (2019). Self-healing evaluation of smart distribution network based on uncertainty theory. IEEE Access, 7, 140022-140029.

[17] Guan, L., Chen, H., & Lin, L. (2021). A multi-agent-based self-healing framework considering fault tolerance and automatic restoration for distribution networks. IEEE Access, 9, 21522-21531.

[18] Moradi, S., Zizzo, G., Favuzza, S., & Massaro, F. (2023). A stochastic approach for self-healing capability evaluation in active islanded AC/DC hybrid microgrids. Sustainable Energy, Grids and Networks, 33, 100982.

[19] Ke, S., Lin, T., Chen, R., Du, H., Li, S., & Xu, X. (2020). A novel self-healing strategy for distribution network with distributed generators considering uncertain power-quality constraints. Applied Sciences, 10(4), 1469.

[20] Jain Tanmay & Verma Kusum. (2024). Reliability Evaluation of Composite Power Systems Integrated with Wind and Solar Energy Sources: A Comprehensive Review. Iranian Journal of Science and Technology, Transactions of Electrical Engineering(2),473-507.

[21] PriyankarRoy,ManishKurre,HariCharan Nannam & AtanuBanerjee. (2023). Reliability evaluation of carrier-based pulse width modulated three-level F-type neutral point clamped inverter with power loss analysis. International Journal of Circuit Theory and Applications(1),162-187.

[22] Usberti Fábio Luiz,Cavellucci Celso & Lyra Christiano. (2023). Interruption flows for reliability evaluation of power distribution networks. Operational Research(1).